POLYMER-PLASTICS TECHNOLOGY AND ENGINEERING
2016, VOL. 55, NO. 17, 1831–1841
http://dx.doi.org/10.1080/03602559.2016.1171875

Taylor & Francis
Taylor & Francis Group

Studies on High Density Polyethylene Reinforced with Phosphate Ore Particles: Thermal, Rheological, Mechanical and Morphological Properties

H. Shaikh[a], A. Anis[a], A. M. Poulose[a], M. Alam[b], M. N. A-Otaibi[c], M. A. Alam[d], and S. M. Al-Zahrani[a]

[a]Chemical Engineering Department, King Saud University, Riyadh, Saudi Arabia; [b]Research Center-College of Science, King Saud University, Riyadh, Saudi Arabia; [c]Material Development, Saudi Basic Industries Corporation, Riyadh, Saudi Arabia; [d]Center of Excellence for Research in Engineering Materials, Advanced Manufacturing Institute, King Saud University, Al-Riyadh, Saudi Arabia

ABSTRACT

Calcareous phosphate ore can be utilized as a cost-effective alternate to other inorganic fillers for polymer-based composites. In this study, composites of high-density polyethylene and phosphate rock ore particles were prepared by melt blending and injection-molding techniques. The thermomechanical, rheological, and mechanical properties of these composites were studied to investigate the effect of filler loading on their functionality. The reduction in the crystallinity of phosphate ore/high-density polyethylene composites was observed compared to that of the neat high-density polyethylene. The relative crystallinity of the neat high-density polyethylene decreases from 53 to 30% by the addition of 2.5–15 wt% of ore, respectively. Comparison of the linear dynamic viscoelasticity for the neat high-density polyethylene and the ore-filled composites shows *t* a monotonic increase in both storage modulus and loss modulus with the increasing frequency. The viscoelastic behavior at high frequencies remains unaffected. However, at lower frequencies, both G' and G'' exhibit diminished frequency dependence. It was also observed that higher filler content decreased the tensile and impact strength, whereas the Young's modulus of the composites increased. The morphological analysis shows relatively weak interaction between the fillers and the matrix because of agglomeration which in turn adversely affects the mechanical properties of the composites.

KEYWORDS

High-density polyethylene; phosphate ore; rheology; tensile properties

GRAPHICAL ABSTRACT

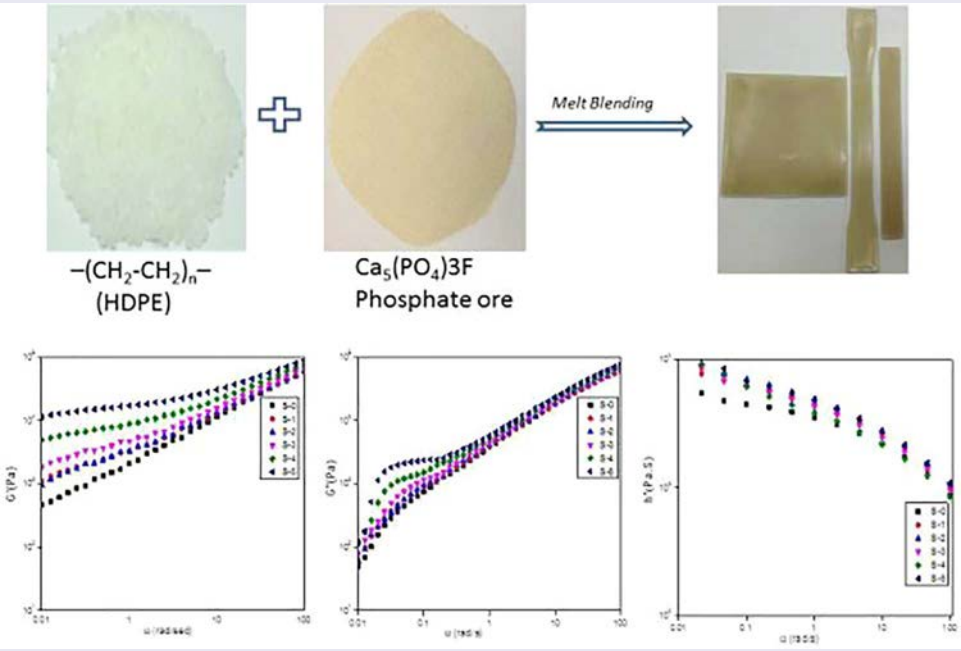

CONTACT H. Shaikh hamshaikh@ksu.edu.sa SABIC Polymer Research Center, King Saud University, P.O. Box 800, Riyadh 11421, Saudi Arabia.
Color versions of one or more of the figures in this article can be found online on at www.tandfonline.com/lpte.

Introduction

Because of its low cost, easy processability, and good mechanical properties the use of high-density polyethylene(HDPE) is continuously expanding in various industrial applications. Over the past two decades, extensive effort has been devoted toward fabricating HDPE-based composites for emerging applications such as conductive thermoplastics, self-healing polyethylene, construction, and biomedical field[1–5]. The formation of composite materials, particularly by melt mixing is an industrially viable option to improve the performance of these thermoplastics and to expand their application.

Various HDPE-based composites are fabricated to study the synergy between the matrix and the characteristics of particular fillers to obtain composites with unique properties. Several methodologies have been used to fabricate various HDPE-based composites, which includes the addition of organic, inorganic, fillers, fibers, etc. Some inorganic fillers such as aluminum diboride, sericite–tridymite–cristobalite, alumina particles, $BaTiO_3$ submicrometer particles, and mica have been attempted.[6–10] Recently, Khalil et al.[11] have prepared HDPE-based composites reinforced by marble sludge particles of different sizes through melt mixing and demonstrated that it is possible to achieve composites with enhanced mechanical properties. Similarly, basalt rock particles have also been used as a filler material in low-density polyethylene matrix to study their mechanical and morphological properties. It was found that the content of basalt filler affects the structural and mechanical properties of the composites. The elongation at break values decrease proportionally with the amount of fillers[12].

The phosphate rocks are naturally occurring form of elemental phosphorus and essential component of fertilizers. It is estimated that about 95% of the total world's phosphate rock is mainly used to produce fertilizers only[13]. Several types of phosphate rocks differ in their chemical, mineralogical, and textural characteristics. Among the known 200 types of phosphate minerals, apatite is the main mineral group for phosphates[14].

Al-Jalamid area, in the North of Saudi Arabia, represents one of the vast calcareous phosphate deposits with a reserve estimation that exceeds 1,000 million tons[15]. This ore typically contains ~25.91% P, 53.13% $CaCO_3$, 1.31% SiO_2, and CaO/P_2O_5 ratio of 2.046[16]. Because of the unique chemical composition of this ore, it can be used as an inorganic filler to fabricate high-performance polymer composites. It is very interesting to see how the complex chemical structure of these ores will interact with particular polymer matrix. There is limited information available in literature studies and need remains to study the influence of these ore particle on the microstructure, mechanical, rheological, and morphological properties of their polymer composites. Here, we have attempted to fabricate phosphate ore particle-reinforced HDPE composites by melt mixing method to study their thermomechanical and rheological properties. The correlation of such properties will provide the useful information about the functionality and processing parameters of such composites. Influence of ore concentration on these composites was also investigated. This article mainly describes the preparation and investigation of structure–property relationship of phosphate ore-based HDPE composites, with an emphasis to explore the possibilities to use these ores as potential inorganic filler.

Materials and methods

High density polyethylene [HDPE: (Hostalen ACP 5331)]

It is an injection and compression molding grade homopolymer polyethylene supplied by TASNEE (The National Industrialization Company, Kingdom of Saudi Arabia). It has a density of 0.953 g/cm^3 and melt flow index (MFI) of 2.1 g/10 min (190°C/2.16 kg) as reported by supplier.

Polybond® 3029

Maleic anhydride-modified high-density polyethylene (PE-g-MA, Polybond 3029, lot OP2B18R000, melt index 4.0 g/10 min at 190°C, 2.16 kg) from Chemtura™ USA was used as a compatibilizer.

Phosphate ore

The phosphate ore samples used in this study was obtained from phosphate deposits in Al-Jalamid, Sirhan Turayf region in Saudi Arabia. The ore particles were crushed using a Denver laboratory ball mill. A dry-sieving was performed using series of selected American Standard Test Method (ASTM) standard sieves. These sieves were arranged in descending order in terms of size and a vertical vibratory sieve shaker was used. The 35 µm ore particles were used as filler to fabricate the composites.

Characteristic of the ore particles

The ore particles were analyzed for particle size distribution (PSD). The measurements were performed using the Microtrac S3500 with the Turbotrac accessory. The powder particles were sprayed through the laser beam path, which causes diffraction of the laser light at different angles depending on the size of the particle, thereby

Table 1. Particle size distribution of the ore particle.

Summary		Percentile	
Data	Value	Size (μm)	% Tile
MV (μm)	34.59	7.16	10
MN (μm)	9.76	9.63	20
MA (μm)	21.50	12.46	30
CS	2.79E-01	15.75	40
SD	11.78	19.10	50
Mz	28.13	22.38	60
σ_i	16.59	25.83	70
Ski	0.2882	30.02	80
Kg	1.447	36.68	90
–	–	45.75	95

obstructing the beam path. The amount and direction of light scattered by the particles was measured by an optical detector array and then analyzed by the Microtrac Software "Micro flex"[17]. Table 1 provides various descriptors of PSD of the ore particles. Figure 1 shows the PSD graph. The peak summary indicates that the average size of the particles is ~19.10 μm.

The density of the untapped ore powder was also measured using a standard volumetric flask of 10 ml volume. The ore powder was filled into the flask exactly parallel to the mark without any tapping. The resultant ore weight was determined and divided by 10 to obtain the density of the ore powder in g/ml. The density of the ore particles is found to be 1.20 gm/ml.

Similarly, the specific surface area of the ore particles was measured with a Tristar-II 3020 (Micromeritics, USA) by nitrogen adsorption/desorption at −196°C. For each analysis, about 0.3 g of sample was first degassed at 250°C under vacuum for 3 h, before analysis, to remove the moisture content from the surface and pores of the particles. The specific surface area of the ore particles was determined from physisorption isotherm data by Brunauer–Emmett–Teller (BET) method. It is found that the BET surface area of ore particles was 5.6883 m^2/g.

Experimental

Preparation of ore/HDPE composite

High-density polyethylene and phosphate ore were dry-blended to obtain composites using an intermeshing, corotating twin-screw extruder (Farrell FTX20, screw dia 26 mm; l/d ratio 35). The screw has got both the dispersive and distributive mixing elements. The dry-blends were fed to the extruder that was operating at a screw speed of 20 rpm and temperatures in different zones were 180, 200, 210, 220, and 220°C. The extruder was cooled, air-dried, and pelletized for further use. The pelletized formulations were injection molded in an Arburg plunger-type injection molder (40 tons, Series SM 120, Asian Plastic Machinery) to obtain specimens of ASTM Type I (D638). Samples with good surface appearance and minimum loss to ore aspect ratio were obtained by optimizing molding parameters such as mold temperature, screw speed, and injection speed.

Table 2 shows the list of different ore/HDPE composites prepared and the neat HDPE resin used in this study. An optimum fraction of ore (2.5–20 wt%) was chosen to obtain various ore/HDPE composites, since at very high concentration of filler the matrix property would be compromised. On the other hand, influence of filler would be suppressed at a too low concentration.

Thermal characterization

Nonisothermal characterization of the neat HDPE resin and ore/HDPE composites was performed by differential scanning calorimetry (DSC, Shimadzu DSC-60). Samples were heated from room temperature to 250°C at a rate of 10°C/min and held at this temperature for 5 min to eliminate any thermal history of the material. Subsequently, the samples were cooled down to 25°C at the same rate as of heating. To observe the melting peak temperature

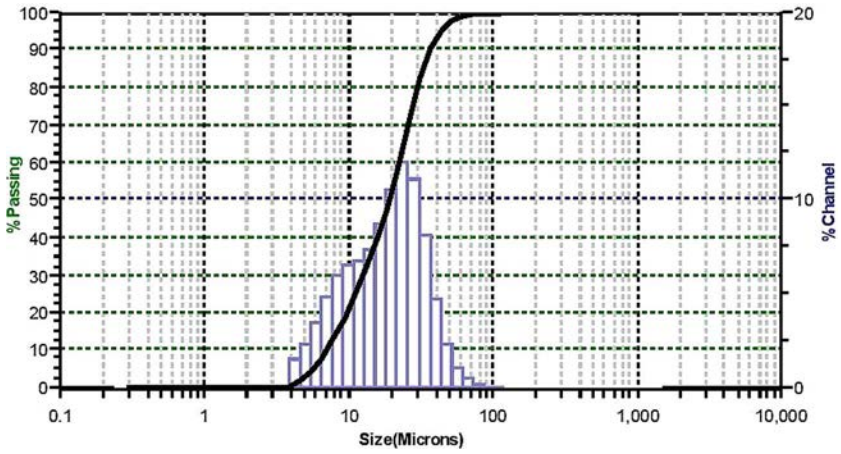

Figure 1. Ore particle size distribution graph.

Table 2. List of ore/HDPE composites prepared in this study.

Samples	Filler	Composition
S-0	HDPE	HDPE (100%)
S-1	Ore	HDPE (92.5%) + PB* (5%) + ore (2.5%)
S-2	Ore	HDPE (90%) + PB (5%) + ore (5%)
S-3	Ore	HDPE (85%) + PB (5%) + ore (10%)
S-4	Ore	HDPE (80%) + PB (5%) + ore (15%)
S-5	Ore	HDPE (75%) + PB (5%) + ore (20%)

PB*: Polybond3029.
HDPE, high-density polyethylene.

after crystallization, the samples were then reheated to 300°C at a rate of 10°C/min. The peak temperature and the area under melting and crystallization curves were recorded to determine melting and crystallization temperatures (T_m and T_c, respectively), and the melting and crystallization enthalpies (ΔH_m and ΔH_c, respectively). Three replicates of measurement were performed and their average values are reported. The degree of crystallinity (X_c) was estimated from the equation below:

$$X_c = 100\Delta H_m/\Delta H_0$$

where ΔH_m is the calculated enthalpy of melting for the composite, ΔH_0 is the theoretical enthalpy of melting for 100% crystalline HDPE with a value of 290.0 J/g[18].

Analysis of mechanical properties

The MFI of HDPE and ore-filled HDPE composite was performed by melt flow indexer (Dynisco Polymer Test, Germany) as per ASTM D1238. The test was performed at 190°C, 2.16 kg.

The tensile properties of the neat HDPE resin and ore/HDPE composite specimens were measured using a Hounsfield H100 KS series tensile testing machine. Dumbbell-shaped ASTM standard samples (Type I for D638) were used for the tests. The tests were performed in a uniaxial tension mode. The notched Izod impact tests were conducted for the measurement of impact strength. The notched specimens of 3 mm thickness with a V-shape notch (depth of the notch 2.7 mm, radius of the notch tip 0.25 mm) were tested with a Multi Impact Tester (Model XJF 22/50) of AMSE, Italy. A hammer speed of 3.5 m/s and pendulum weight of 0.818 kg were chosen for the measurement at 23°C, according to ASTM D256. The samples were dried overnight at 90° C and allowed to cool at room temperature before testing. For each specimen, at least five measurements were performed and their mean value was reported.

Rheological analysis

The viscoelastic properties of the control and the prepared composites were analyzed using AR-G2 Rheometer (TA instruments, USA). The samples were compression-molded to obtain specimen with required diameter that can fit in the circular plates of the rheometer. The linear viscoelastic measurements were performed for melts at 190°C using the parallel plate geometry (diameter 25 mm and gap of 1,000 µm). Dynamic frequency sweeps were performed from 0.1 to 100 rad/s range at a strain within the linear viscoelastic region of the materials. The strain was kept constant at 0.01% over the whole frequency range to ensure linearity. This strain was selected from a dynamic strain sweep test, which was performed from 0.0001–10% strains at a fixed frequency of 1 Hz and the deviation strain from linearity was tracked. The frequency sweep test was performed at constant temperature. Additionally, time sweeps were also performed to ensure that no thermal degradation taking place and the material is stable during the length of measurement. The temperature was stable within 0.5°C over the range used in this study. Each measurement was performed on a fresh sample and repeated measurements had been conducted to ensure the reproducibility of the experimental results.

Wide-angle X-ray diffraction analysis

Wide-angle X-ray diffraction (XRD) analysis was performed to investigate the crystalline behavior of the ore particles–HDPE composites. The injection-molded specimens were used for the XRD analysis. A 2θ from 5° to 50° in reflection mode was scanned at 5°/min. A computer-controlled wide-angle goniometer coupled to a sealed-tube source of Cu Kα radiation ($\lambda = 1.54056$ Å) was used. The polyethylene (PE) crystalline thickness perpendicular to the reflection plane L_{hkl} was obtained according to Scherrer's equation

$$L_{hkl} = \frac{\lambda K}{\beta \cos\theta}$$

where

K = Scherrer constant or the shape factor of crystalline thickness (0.9)

λ = Wavelength of X-ray (1.54056 Å)

θ = Incident angle (Half of 2θ value)

β = FWHM is the full-width at half-maximum, and the X_c of polyethylene was determined from the following equation:

$$X_c = \frac{I_{100} + 1.46I_{200}}{I_{100} + 1.46I_{200} + 0.75I_{\alpha}} \times 100\%$$

where I_{110}, I_{200}, and I_{α} are the integral areas of the (1 1 0), (2 0 0), and the amorphous peak of polyethylene, respectively[19].

Morphological analysis

The morphological characterizations of ore/HDPE composite were performed by scanning electron microscopy (SEM, Model JEOL JSM-6360A). The cryogenic morphological analysis was performed on the specimens taken from injection-molded bars (Type I for D638) of neat HDPE and ore/HDPE composites. A small V-shaped notch was applied on the specimen followed by their fracture in liquid nitrogen. The freeze-fractured surfaces were then observed under the SEM. All the samples were gold-sputtered before observation. The TEM imaging was performed using a JEM-1400 (JEOL) field-emission electron microscope operating at an accelerating voltage of 120 kV.

Results and discussion

Figure 2 shows the dynamic thermogram (heating andcooling) of neat HDPE resin and the ore/HDPE composites. Table 3 summarizes their nonisothermal crystallization parameters. The endothermic peak of neat HDPE appears at around 134.50°C and increases gradually for the ore/HDPE composites with the increasing filler concentration. In the HDPE/ore composites, the melting endotherm decreases in size and T_m increases with an increase in filler amount as shown in Figure 1. This is attributed to the fact that during the cooling of HDPE matrix, the melt nucleates on the surface of the filler at relatively high temperature and forms crystal lamellas with larger thickness, resulting in high T_m[20]. The increases in crystal size of composites were also observed in the XRD analysis. The increase in T_m is also because the fillers dispersed in the HDPE matrix shield the conduction of heat to the crystallites until at higher temperatures; the heat flow is enough to melt down the crystallites[21]. The enthalpy of melting (ΔH_m) decreases proportionally with the amount of filler, however, the enthalpy of melting ΔH_m is sensitive to several factors such as previous thermal history, impurities, presence of filler, and structural imperfections resulting from processing. This thermal behavior could be attributed to the fact that the ore decreases the crystalline structure as well as melt viscosity of the HDPE. However, it is interesting to observe that sample S-5 shows a more significant influence over the thermal property of the composites. This may be attributed to the large content of the filler. The high amounts of fillers contribute to a more nucleation sites, thereby demonstrating a greater effect on thermal behavior.

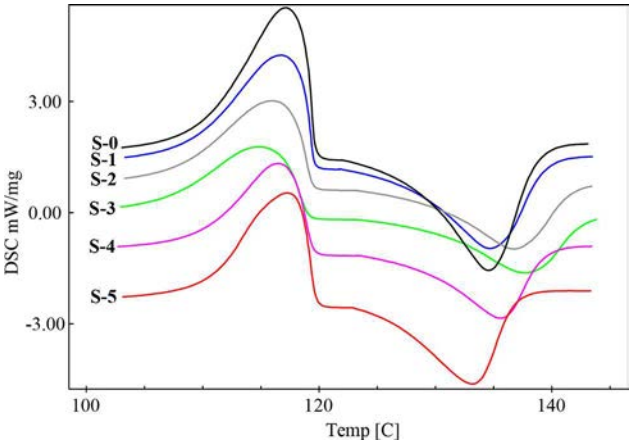

Figure 2. Exothermic and endothermic thermograms of the neat HDPE resin and ore/HDPE composites. *Note*: HDPE, high-density polyethylene.

There is a gradual decrease in T_c value of the samples from S-1 to S-4 composites except for S-5 for which it was to found increase. This can be attributed to the fact that the increased concentration of ore particles causing a heterogeneous nucleating effect. Similarly, ΔH_c decreased for samples S-1 to S-4; however, there was a significant increase in enthalpy of crystallization (ΔH_c) for S-5 indicating the imperfect crystallization for the composite of relatively higher filler concentration.

In general, the reduction in the crystallinity of the composites was observed compared to neat HDPE. The crystallinity of HDPE decreased from 53 to 30% with an increase in filler content from 2.5 to 15 wt%, respectively. This may be because of large amounts of ore particles locating themselves in the interlamellar spaces, leaving a little room for additional crystallization, which results in decrease in crystallinity. This phenomenon between reinforcing fillers and HDPE matrix has been reported in the literature studies[22,23] and is in agreement with the XRD results.

Table 3. Thermodynamic properties of neat HDPE and phosphate ore/HDPE composites.

Samples	T_m (°C)	T_c (°C)	ΔH_c (J/g)	ΔH_m (J/g)	X_c (%)
S-0	134.73 ± 0.20	117.04 ± 0.89	173.21 ± 1.11	156.22 ± 0.87	53.86 ± 2.16
S-1	134.93 ± 0.35	116.66 ± 0.45	131.03 ± 1.88	119.85 ± 0.30	41.32 ± 2.03
S-2	135.53 ± 0.55	115.93 ± 0.30	118.61 ± 0.75	97.79 ± 2.25	33.72 ± 1.38
S-3	136.63 ± 0.60	114.75 ± 0.15	102.71 ± 1.30	89.97 ± 1.05	31.02 ± 1.80
S-4	135.88 ± 0.12	114.45 ± 0.65	99.41 ± 1.49	88.37 ± 1.18	30.47 ± 1.51
S-5	136.96 ± 1.10	117.36 ± 1.06	126.57 ± 1.18	110.28 ± 2.64	38.02 ± 1.10

HDPE, high-density polyethylene.

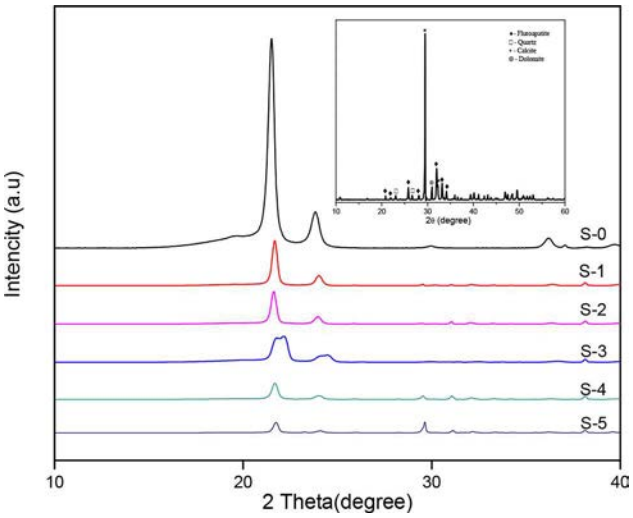

Figure 3. XRD diffractograms of the neat HDPE resin and ore/HDPE composites (inset pure ore XRD pattern). *Note*: XRD, X-ray diffraction; HDPE, high-density polyethylene.

Wide-angle X-ray diffraction analysis

The XRD patterns, having 2θ of 5–50°, for pure HDPE, ore particles, and reinforced HDPE composites with 2.5, 5, 10, 15, and 20 wt% ore content are shown in Figure 3. It is well known that the crystal structures of polyethylene are monoclinic, orthorhombic, and hexagonal depending on the processing conditions[24]. In the observed XRD spectra of neat HDPE, one strong peak appearing at 21.5° and two moderately strong peaks at 23.8° and 36.5° shows interplanner spacing of 3.9612, 3.636, and 2.480 Å, respectively. These peaks correspond to the (1 1 0), (2 0 0), and (0 2 0) lattice planes with orthorhombic structure[25]. The XRD diffractogram of phosphate rock particles shows the various peak of fluorapatite [$Ca_{10}(PO_4)\ 6\,F_2$] in the 2θ of 25.80°, 32.22°, 33.56°, 33.80°, 46.65°, and 49.67°; calcite ($CaCO_3$) at 2θ of 29.34°, 35.50°, and 39.86°; dolomite [$CaMg\ (CO_3)_2$] peak position at 2θ of 31.02°, 41.27°, and quartz (SiO_2) at 2θ of 26.86°, 40.37°[26].

The XRD profile of ore/HDPE composites shows similar pattern to that of neat HDPE. The peak position remains unchanged, while the intensity and width of each peak varies depending on the samples. This is the indication of change in crystallinity and crystallite size in the samples. Further, the intensity of the peaks corresponding to (1 1 0) and (2 0 0) planes for each sample are analyzed, and the data of crystalline thickness and crystallinity are summarized in Table 4. From this data, it was observed that the crystal size increases, while the crystallinity decreases with the increasing amount of filler content. This fact also supported by DSC analysis. It can also be noted that the peak position of two HDPE peaks are slightly shifted to higher angle,

Table 4. XRD properties of neat HDPE and phosphate ore/HDPE composites.

	2θ (°)		FWHM		Crystal size (A°)		%
Samples	(110)	(200)	(110)	(200)	(110)	(200)	Crystallinity
S-0	21.502	23.829	0.384	0.467	234.9	193.2	49.25
S-1	21.679	24.020	0.361	0.394	284.8	229.1	47.65
S-2	22.015	24.353	0.365	0.857	203.9	206.4	44.33
S-3	21.624	23.963	0.326	0.408	275.7	221.4	43.96
S-4	21.683	24.014	0.361	0.442	248.8	204.1	43.55
S-5	21.714	24.072	0.306	0.381	293.7	237.00	46.70

XRD, X-ray diffraction; FWHM, full-width at half-maximum; HDPE, high-density polyethylene.

which can be because of the unit cell distortion of HDPE because of filler addition. Similar phenomenon has been reported in other HDPE-based composites[27].

It was also noticed that the sample S-5 shows the characteristic of blend of HDPE and ore particles that is because of the high amount of ore particles. These ore particles mainly contain calcite in higher fraction; therefore the calcite peak appears at 2θ at 29.34° and clearly visible in the composite sample. The appearance of the distinct characteristic peaks of the matrix and the filler clearly revealed the noninterference of crystal planes indicating no chemical or phase transformation interactions took place in the composites.

Rheological analysis

Rheology is a useful tool to study the viscoelastic behavior of materials that govern their mechanical properties. Figure 4 shows the variation of complex viscosity with frequency for the ore/HDPE composites.

It is well-known fact that the addition of filler to the polymer matrix increases the viscosity of the melt. The rigid ore particles may disturb the flow and provide an

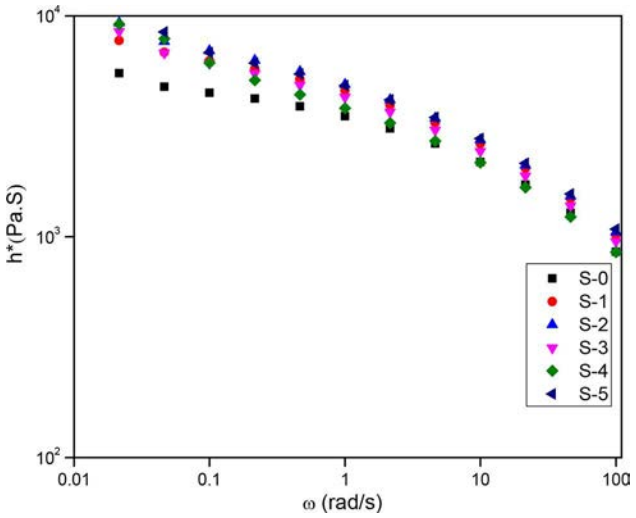

Figure 4. The variation of complex viscosity with frequency for the ore/HDPE composites. *Note*: HDPE, high-density polyethylene.

obstruction to flow of the polymer melt, thus causing an increase in viscosity. The increase in viscosity depends on the various factors such as concentration, PSD, and shape of the fillers. The highest complex viscosity was observed for the composite with highest filler loading. In addition, the presence of agglomerates because of high filler loading may cause resistance toward the flow and increases the viscosity of the composites. It was observed that at 0.1 rad/s the complex viscosity of neat HDPE is 4491 Pa.s while that of 20 wt% ore/HDPE samples is about 6,821 Pa.s, respectively.

However, complex viscosity found to decrease with the increasing shear rate (frequency) in all samples. It is observed that at 100 rad/s the complex viscosity of neat HDPE is about 853 Pa.s while that of 20 wt% ore/HDPE samples is 1,081 Pa.s, respectively. This indicates that the ore particles exhibits shear thinning behavior (pseudo plasticity). It may also because of the increase number of polymeric chain entanglements being broken than the new entanglements being reformed. This phenomenon also observed in other HDPE-based composites[28,29].

Strain sweep test

Figure 5 shows the strain sweep test of ore/HDPE composites. It is observed that the response of all the composite samples depend on the applied strain. The sample with lower filler loadings (S-1 and S-2) shows similar behavior to that of the neat HDPE. All samples, up to 0.01% strain, show the constant plateau for storage modulus G' and exhibit the linear viscoelastic region. However, above these range, composites of higher filler loading (S-3 to S-5) shows drastic changes in storage modulus G'. The storage modulus decreases sharply for these composites because of the changes in composite structure. It is interesting to note that the strain at which the storage modulus sharply dropped down differs with the concentrations of the filler particles. This can be attributed to the difference in PSD of the ore particles. This phenomenon with HDPE-based composites has been previously reported in literature studies[30]. With the increasing strain, a reduction in the storage modulus G' occurs because of the breakage of the composite structure. At high dynamic strain, the breaking of composite structure can be attributed to the incompatibility and poor adhesion between the matrix and the fillers. Also, increasing the strain generates high shear stresses that may not be sufficiently transferred through the interface, and the deformation energy cannot be effectively absorbed by the filler particles[31].

Figure 6 shows the variation of the storage modulus versus frequency. It is observed that the storage modulus for the composites is higher than that of neat HDPE. The formation of polymer–filler network causes the change in the storage modulus. The storage modulus at 0.1 rad/s of neat HDPE is 460.9, 1,103 GPa for S-1, 937.8 GPa for S-2, 1,846 GPa for S-3, 4,867 GPa for S-4, and 11,190 GPa for S-5. As frequency increases, the storage modulus differences decreases between the composites. The storage modulus behavior indicates the ability to store the energy because of the external forces which were observed to increase with increasing angular frequency (ω) for all the composites. This behavior can be attributed to the intrinsic rigidity and agglomeration of the ore particles. It should also be noted that addition of filler might lead to changes in the relaxation time spectrum resulting in changes in viscoelastic properties of the composites.

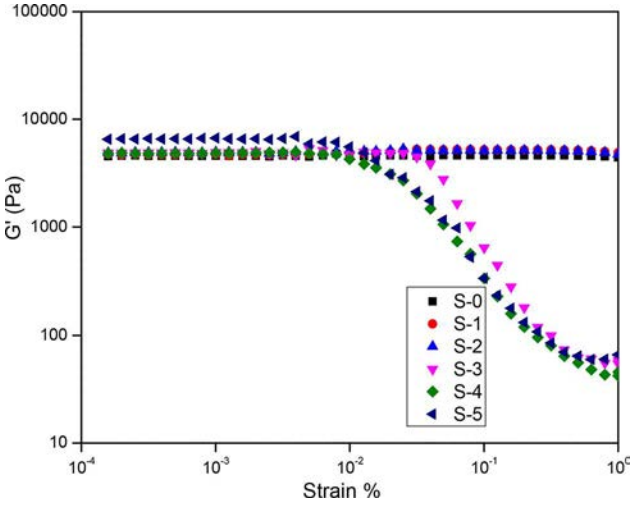

Figure 5. Strain sweep test of ore/HDPE composites. *Note*: HDPE, high-density polyethylene.

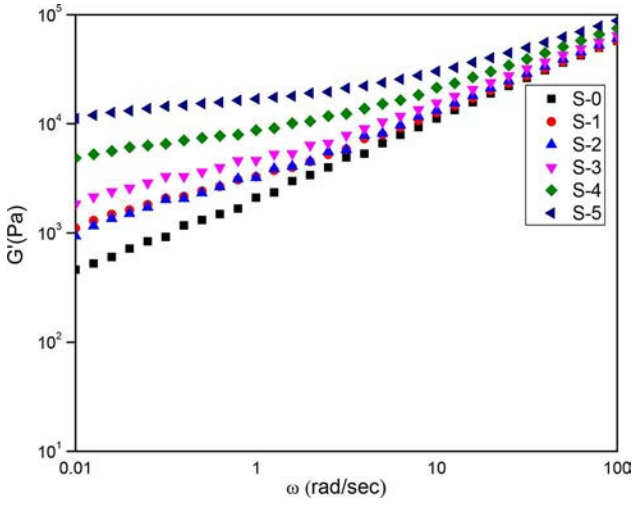

Figure 6. The storage modulus versus frequency for HDPE and ore/HDPE composites. *Note*: HDPE, high-density polyethylene.

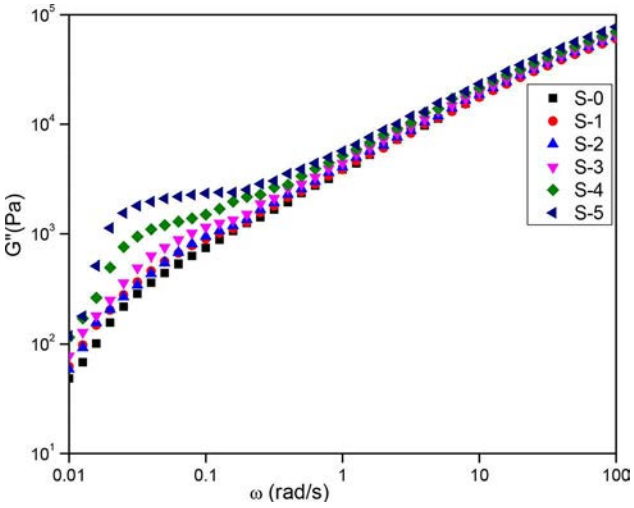

Figure 7. The loss (G'') modulus with frequency (ω) for ore-filled HDPE composites. *Note*: HDPE, high-density polyethylene.

Figure 7 shows the variation of the loss (G'') modulus with frequency (ω) for ore-filled HDPE composites. It has been observed that the loss modulus also increases with an increase in frequency for all the samples. The loss modulus at 0.1 rad/s is 741, 895.6, 942.6, 1,154, 1,499, and 2,342 GPa for S-0, S-1, S-2, S-3, S-4, and S-5, respectively. At lower frequency, the composites show greater ability toward impact absorption. The difference in loss modulus of the composites can be attributed to their PSD. As frequency increases, the loss modulus difference decreases between the composites. A higher number of particles result in more particle–particle interaction that causes more resistance to flow. As the shear rate increases, this effect became relatively weak and eventually breaks down at high shear rates. Thus, the viscoelastic behavior at high frequencies remains unaffected by the addition of the filler particles. However, at lower frequencies, both G' and G'' exhibit frequency dependence characteristics. Similar behaviors of HDPE-based composites have also been reported[32,33].

Analysis of mechanical properties

Figure 8 shows the MFI plot of the HDPE and ore/HDPE composites. It was observed that the MFI decreases gradually with the increasing filler loading. This is because of a perturbing polymer chain motion because of the presence of the filler. The results show that the neat HDPE has higher MFI values compared to that of the ore/HDPE composites. It can be deduced that lower filler loadings result in a better interaction with the matrix. It could be seen that 2.5 wt% filler improved the rigidity of the HDPE composites, followed by 5, 10, 15, and 20 wt%. As the MFI is a direct measure of a material's viscosity, these results indicates that the presence of ore filler reduces the viscosity of the HDPE matrix.

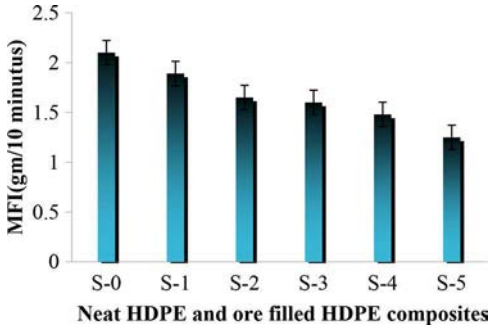

Figure 8. MFI plot of neat HDPE and ore/HDPE composites. *Note*: MFI, melt flow index; HDPE, high-density polyethylene.

Impact strength is an important property that gives an indication of overall toughness of the material. A material breaking under an impact is caused by rapid crack propagation. The propagation rate of cracks is inversely proportional to the material's impact strength. The impact strength of the filler-reinforced composite depends on filler rigidity, interfacial stress resistance, and filler aspect ratio. Table 5 shows the mechanical properties of the neat HDPE and ore-filled HDPE composites. It was observed that the impact strength of the composites is lower than that of neat HDPE. The impact strength values of the ore-filled HDPE composites decreased proportionally with the increasing ore content. Thus, increasing the content of the filler probably increased the level of stress concentration in the composites. The impact may be propagated rapidly along the filler–polymer interface because of the

Table 5. Mechanical properties of neat HDPE and ore/HDPE composites.

Samples	Young's modulus (MPa)	Tensile strength (MPa)	Tensile elongation at yield (%)	Impact energy (Joule)	Impact strength (kJ/m^2)
S-0	515.30	22.3 (±0.6543)	9.83 (0.4163)	0.57 (0.1014)	18.45 (1.1651)
S-2	722.66	21.11 (±0.6506)	9.06 (0.7023)	0.47 (0.0750)	17.95 (0.3968)
S-3	737.92	20.10 (±0.7399)	8.63 (1.0211)	0.41 (0.0757)	16.32 (0.9400)
S-4	710.94	20.92 (0.4532)	8.46 (1.3012)	0.42 (0.1553)	13.58 (0.8086)
S-5	756.84	18.78 (0.4158)	7.50 (1.0066)	0.38 (0.1665)	11.10 (1.5419)
S-6	1014.1	19.44 (1.2035)	8.5 (0.8717)	0.28 (0.0650)	9.70 (0.8792)

HDPE, high-density polyethylene.

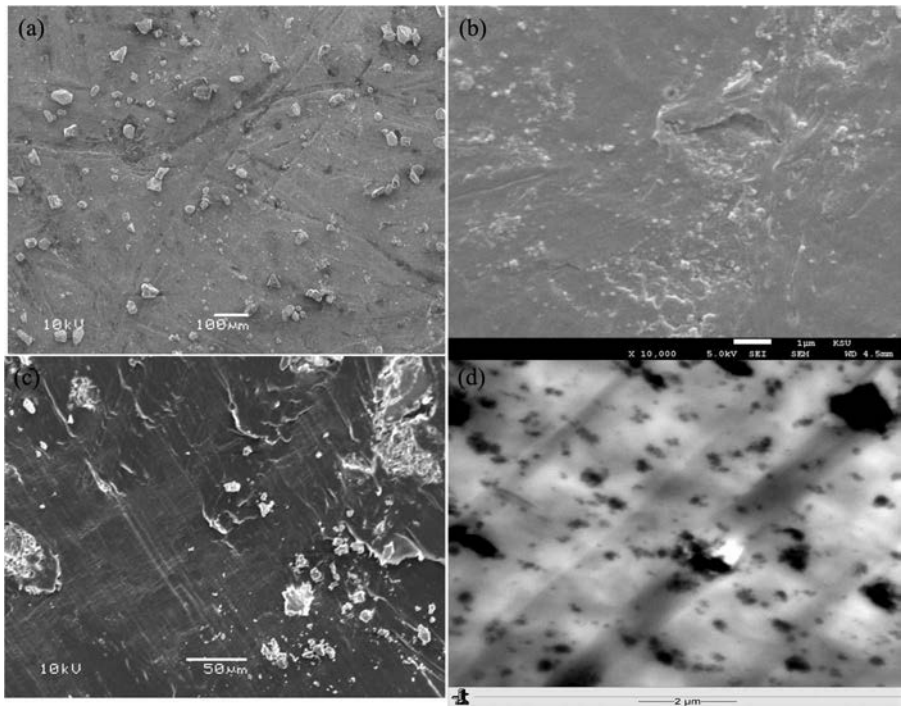

Figure 9. The SEM micrograph of (a) ore particle, (b) 2.5 wt% ore-filled HDPE composite, (c) 15 wt% of ore-filled HDPE composite, and (d) TEM image of 15 wt% of ore-filled HDPE composite. *Note*: SEM, scanning electron microscopy; HDPE, high-density polyethylene.

induction of fissures because of the relatively weak adhesion between the two phases. Similar results were observed in Fe powder-reinforced high-density polyethylene composites[34].

Similarly, it is observed that the tensile strength and percent elongation at yield decreased gradually with the increasing ore content of the composites. The reduction of these properties in ore-filled HDPE composites can be attributed to the weak interfacial adhesion between the fillers and the matrix. On the other hand, increase in Young's modulus was observed with the increasing filler content; this can be attributed to stiffer nature of the ore particles. Similar behavior was observed in other types of fillers in HDPE composites[35,36].

Morphological analysis

Transmission Electron Microscopy (TEM) and SEM images of surface (cryo-fractured) of phosphate ore filler and HDPE composites are shown in Figure 9(a–d). In ore/HDPE composites of lesser content of ore, 2–5 wt% were found to be well distributed. On the other hand, for ore of relatively larger amount, the distribution of fillers in polymer matrix is rather random and aggregation of filler takes place. It is evident from the analysis that phosphate ore-filled HDPE composites exhibited weak adhesion at the polymer–filler interface.

Conclusion

The present study demonstrates that the phosphate ore particles can be used as reinforcing filler in HDPE composites. It has been found that the ore filled-HDPE shows considerable modifications in the physical and mechanical properties compared to neat HDPE. The ore particles when added to HDPE improved its rigidity but appreciably decreased the MFI, strength, and elongation at yield because of the agglomeration of ore particles and weak adhesion between the filler and the matrix. The SEM and TEM micrographs also show the agglomeration of the ore particles. The impact strength decreased gradually with the increasing amount of ore content because of the reduction in elasticity of the composites, thereby reducing the deformability of the matrix. Also, clearly loading of the filler content has an important effect on the properties of the composites, which can be improved by altering particle size and use of a better compatibilizer.

Conflict of interest

The authors declared that there is no conflict of interest regarding the publication of this paper.

Funding

The authors would like to extend their sincere appreciation to the Deanship of Scientific Research at King Saud University

for its funding of this research through the Research Group Project No. RGP-095.

References

[1] Yuan, Q.; Bateman, S.A.; Dongyang, W. Mechanical and conductive properties of carbon black-filled high-density polyethylene, low-density polyethylene, and linear low-density polyethylene. J. Thermoplast. Compos. Mater. **2010**, *23*, 459–471.

[2] Shaikh, H.M.; Gulrez, S.K.H.; Anis, A.; Poulose, A.M.; Qua, P.E.H.; Yadav, M.K.; Al-Zahrani, S.M. Progress in carbon fiber and its polypropylene- and polyethylene-based composites. Polym. Plast. Technol. Eng. **2014**, *53*, 1845–1860.

[3] Mao, D.; Lee, R.F.; Yaniv, Z. Self-healing polyethylene **2014**, WO 2014081930.

[4] Lu, N.; Korman, M.T. Engineering sustainable construction material: Hemp-fiber-reinforced composite with recycled high-density polyethylene matrix. J. Archit. Eng. **2013**, *19*, 204–208.

[5] Balakrishnan, H.; Husin, M.R.; Wahit, M.U.; Abdul Kadir, M.R. Preparation and characterization of organically modified montmorillonite-filled high density polyethylene/hydroxyapatite nanocomposites for biomedical applications. Polym. Plast. Technol. Eng. **2014**, *53*(8), 790–800.

[6] Sava, Ö.; Ficicib, F.; Kayikcib, R.; Köksal, S. Investigation of mechanical and dry sliding wear behaviours of ALB_2/PE polymer matrix composites. Acta Phys. Pol. **2014**, *125*, 388–390.

[7] Ping, F.; Pengbo, L.; Huawei, Z.; Berenika, H.; Wen, X. Effect of interfacial interaction on properties of gamma ray-irradiated high density polyethylene reinforced by sericite-tridymite-cristobalite. Polym. Plast. Technol. Eng. **2009**, *48*, 327–332.

[8] Mohammad, T.H.M.; Alireza, B.; Samaneh, S. Influence of alumina particles on thermal behavior of high density polyethylene (HDPE). Polym. Plast. Technol. Eng. **2012**, *51*, 214–219.

[9] Gonzalez, B.J.; Martinez, T.J.; Sepúlveda García, M.E.; Portillo, R.A.; Gonzalez, G.G. Composites based on HDPE filled with $BaTiO_3$ submicrometric particles. Morphology, structure and dielectric properties. Polym. Test. **2013**, *32*, 1342–1349.

[10] Liang, J.Z.; Yang, Q.Q. Mechanical, thermal, and flow properties of HDPE—mica composites. J. Thermoplast. Compos. Mater. **2007**, *20*, 225–236.

[11] Khalil, A. Synergistic effect of industrial waste in high density polyethylene. J. Mater. Environ. Sci. **2014**, *5*, 849–858.

[12] Akinci, A. Mechanical and morphological properties of basalt filled polymer matrix composites. Arch. Mater. Sci. Eng. **2009**, *35*, 29–32.

[13] Abouzeid, A.Z.M. Physical and thermal treatment of phosphate ores-an overview. Int. J. Miner. Proc. **2008**, *85*, 59–84.

[14] Meck, M.L.; Atlhopheng, J.; Masamba, W.R.L.; Ringrose, S.; Diskin, S. Minerals that host metals at Dorowa rock phosphate mine, Zimbabwe. Open Mineral. J. **2011**, *5*, 1–9.

[15] Riddler, G.P.; Eck, M.V.; Aspinall, N.C.; McHugh, J.J.; Parker, T.W.H.; Farasani, A.M.; Dini, S.M. Saudi Arabian deputy ministry for mineral resources, Jeddah, technical record RF-TR-06-2, **1986**.

[16] Arafat, Y.; Al-Fariss, T.F.; Muhammad, A.N. A bench scale study on the enrichment of Saudi phosphate rock used for H_3PO_4 production, Proceedings of the International Conference on Chemical Engineering and Materials Science (CEMS '14), Venice, Italy, March 15–17, 2014; pp. 125–129. (www.europment.org/library/2014/venice/BICHE.pdf)

[17] Philip, P.E. Particle size measurement of cement by laser diffraction using Microtrac S3500, SL-AN-26 Revision A, 2008, www.Microtrac.com (accessed 2016).

[18] Medel, F.J.; García-Álvarez, F.; Gómez-Barrena, E.; Puértolas, J.A. Microstructure changes of extruded ultra high molecular weight polyethylene after gamma irradiation and shelf-aging. Polym. Degrad. Stab. **2005**, *88*, 435–443.

[19] Alamo, R.G.; Mandelkern, L. Thermodynamic and structural properties of ethylene copolymers. Macromolecules. **1989**, *22*, 1273–1277.

[20] Gray, D.G. "Transcrystallization" induced by mechanical stress on a polypropylene melt. J. Polym. Sci. Polym. Lett. Ed **1974**, *12*, 645–650.

[21] Frounchi, M.; Dourbash, A. Oxygen barrier properties of poly(ethylene terephthalate) nanocomposite films. Macromol. Mater. Eng. **2009**, *294*, 68–74.

[22] Kamini, S., Maiti, S.N. Crystallization and melting behavior of HDPE in HDPE/Teak wood flour composites and their correlation with mechanical properties. J. Appl. Polym. Sci. **2010**, *118*, 2264–2275.

[23] Pimpatima, P.; Ekrachan, C.; Piyasan, P.; Bunjerd, J. Polyethylene/clay nanocomposites produced by in situ polymerization with zirconocene/MAO catalyst. J. Nanomater. **2013**: Article ID 154874, p 9 http://dx.doi.org/10.1155/2013/154874

[24] Basset, D.C. Chain-extended polyethylene in context: A review. Polymer **1976**, *17*, 460–470.

[25] Yijian, L.; Weichuan, D.; Demin, T.; Wei, Z.; Qiangguo, D. Space charge distribution and crystalline structure in low density polyethylene (LDPE) blended with high density polyethylene (HDPE). Polym. Int. **2005**, *54*, 465–470.

[26] Abdallah, A.; Abdalazeem, A.; Mustafa, A. Qualitative and quantitative analysis of phosphate rock from Hazm Al-jalamid area, northern Saudi Arabia. Int. J. Basic Appl. Sci. **2014**, *3*, 190–198.

[27] Sami, A.; David, E.; Frechette, M. Procedure for evaluating the crystallinity from X-ray diffraction scans of high and low density polyethylene/SiO_2 composites, Electrical Insulation and Dielectric Phenomena (CEIDP), 2010 Annual Report Conference 2010. doi:10.1109/CEIDP.2010.5724069:1-4.

[28] Li, T.Q.; Wolcott, M.P. Rheology of wood plastics melt. Part 1. Capillary rheometry of HDPE filled with maple. Polym. Eng. Sci. **2005**, *45*(4), 549–559. doi:10.1002/pen.2030834,35

[29] Hornsby, P.R. Rheology, compounding and processing of filled thermoplastics. Adv. Polym. Sci. **1999**, *139*, 155–217.

[30] Anselm, O.O.; Joseph, N.A.; Nduji, A.A. Characterization and comparison of rheological properties of agro fiber filled high-density polyethylene bio-composites. Open J. Polym. Chem. **2014**, *4*, 12–19.

[31] Aranguren, M.J.; Mora, E.; DeGroot, J.V.; Macosko, C.W. Effect of reinforcing fillers on the rheology of polymer melts. J. Rheol. **1992**, *36*, 1165–1182. doi:10.1122/1.550306
[32] Youhong, T.; Cheng, Y.; Ping, G.; Lin, Y.; Chengbi, Z.; Wei, L. Rheological study on high-density polyethylene/organoclay composites. Polym. Eng. Sci. **2011**, *51*, 133–142.
[33] Chandran, G.V.; Waigaonkar, S.D. Rheological and dynamic mechanical characteristics of rotationally moldable linear low-density polyethylene fumed silica nanocomposite. doi:10.1002/pc.23496
[34] Gungor, A.J. The physical and mechanical properties of polymer composites filled with Fe powder. Polym. Sci. **2006**, *99*, 2438–2442.
[35] Münir, T.; Gülsoya, O.H. The mechanical and morphological properties of HDPE composites filled with SiO_2, ZNO, $Mg(OH)_2$ and $CaCO_3$ nano powder. Rom. J. Mater. **2013**, *43*, 417–424.
[36] Nicoleta, R.S.; Daniela, R. Mechanical and thermal properties of zinc powder filled high density polyethylene composites. Polym. Test. **2001**, *20*, 409–417.